Analysis of the effects of intraocular lens edge design on dysphotopsia for pseudophakic patients

Meimei Kong (孔梅梅)[1], Zhishan Gao (高志山)[1], Xinhua Li (李新华)[1], Changzheng Huang (黄长征)[2], Ru Zhang (张 茹)[2], and Weihong Xiao (肖蔚鸿)[2]

[1]*School of Optical Engineering, Nanjing University of Science and Technology, Nanjing 210094*

[2]*ABLE Eye Device CO. Ltd., Zhengzhou 450001*

The dysphotopia that is connected to the reflection of light from the intraocular lens (IOL) edge is analyzed. A new IOL with "Σ" edge is investigated, and other three IOLs are also studied for comparison. The interaction of rays as a function of edge design was evaluated in an experimental model of the pseudophakic eye using the ray-tracing program of ZEMAX software (Focus Software, Inc.). The results show the rays crossing the edges of IOLs form an image with the shape of a partial ring or thin arc in the periphery of the retina, the potential of the "Σ" edge to lower dysphotopsia for pseudophakic patients is promising.

OCIS codes: 170.3880, 170.4460, 220.2740.

At present, the optimal method to treat cataract is cataract extraction with implantation of an intraocular lens (IOL). But after the cataract surgery, posterior capsule opacification (PCO) and dysphotopsia affect the quality of vision frequently.

PCO, mostly, is formed by the proliferation and migration of rudimental lens cells (LECs) across the posterior capsule[1]. Appropriate IOL edge design may play a role in preventing PCO. Many studies have shown that a sharp, square IOL edge, which creates a discontinuous bend in the posterior capsule, can impede the migration of LECs[2−6]. However, some patients with square-edged IOLs often describe unwanted light images, such as flashes, arcs, halos, or sprinkles of light and are usually encountered in scotopic light conditions under which the iris dilates. These adverse light-related visual phenomena can be called dysphotopia[7].

It has been established that the dysphotopia is connected with the reflection of light from the IOL edge: patients who receive an IOL with flattened edges will be at increased risk of experiencing unwanted images associated with edge reflections than those who received round-edged IOLs[8,9].

A new IOL with sunken edge is studied in this letter (Fig. 1(a)). Its optical design is an equal-biconvex design with 14.971 mm anterior and posterior radius curvature, and its sunken edge, which induces migration of LECs to the hollow, may prevent PCO. This IOL is called "Σ"-IOL because the sunken edge looks like the Greek letter "Σ" from the profile. The other three IOLs are also studied for comparison (Figs. 1(b), (c), and (d)): two square-edged designs (square-edged 1 and square-edged 2), a round anterior edge and a square posterior edge design (round-/square-edged). The material of these IOLs is polymethyl-methacrylate(PMMA), and they are made in ABLE Eye Device CO. LTD, China.

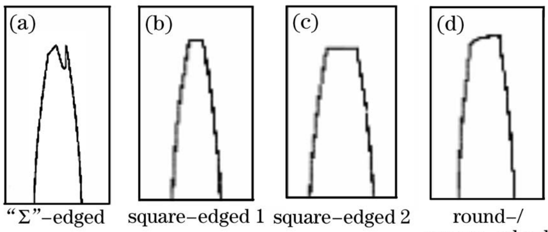

Fig. 1. Shape of IOL.

The interaction of rays as a function of edge design is evaluated in an experimental model of the pseudophakic eye using the ray-tracing program of ZEMAX software (Focus Software, Inc.). The experimental model eye is shown as Fig. 2, and the physiological parameters were: corneal power, 42 diopters (D); anterior chamber depth, 4.55 mm; IOL power, 20 D; optical diameter, 5.5 mm; axial length, 23 mm; pupil diameter, 5.5 mm; the sunken angle of "Σ"-edged, 17 degree. The glare source is placed at a 35 degree angle to the optical axis because it has been demonstrated that this angle maximizes the intensity of the reflected image created by squared edges and so the dysphotopia is distinct[10].

The stray lights, which may induce dysphotopsia in the retina, are found with non-sequential ray tracing method. Based on the propagation characteristics of the stray rays, these ray paths are ascertained respectively for above four edge designs: one type ray path is shown in Fig. 3, where the rays hitting the square edges of the three IOLs may cause unwanted light images on the side of the retina; the special type ray path induced by the "Σ"-edged is shown in Fig. 4, where the rays are reflected by the edge to the cornea, then reflected by the

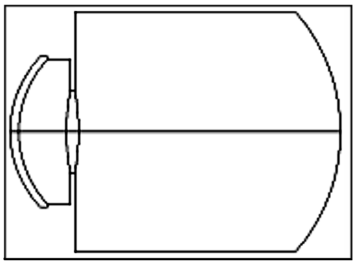

Fig. 2. Experimental model of a pseudophakic eye.

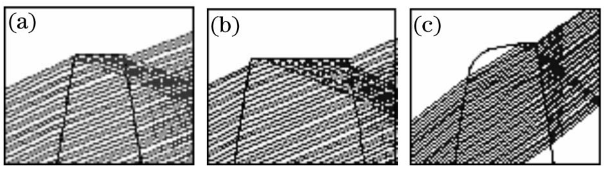

Fig. 3. Ray tracing through square-edged 1 (a), square-edged 2 (b), and round-/square-edged (c).

cornea again, and at last arrived at the retina, which may cause dysphotopsia.

For each design, in order to ensure accurate peak intensity, spatial location and energy distribution of the dysphotopsia image, 160000 rays from a glare source through the pseudophakic eye model are traced. The defaulted intensity of incident glare source is supposed to be 1 W. The retinal images and energy distributions formed by square-edged design (Fig. 5), round-/square-edged design (Fig. 6) and "Σ"-edged design (Fig. 7) are shown as following. In the Figs. 5–7, the coordinate system is described for x and y on the image plane of retina, the origin is at the intersection of optical axis with the retina (unit: mm).

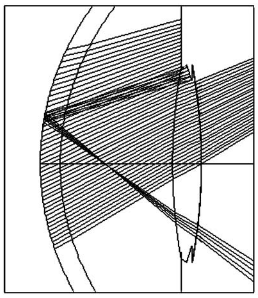

Fig. 4. Ray tracing through "Σ"–edged.

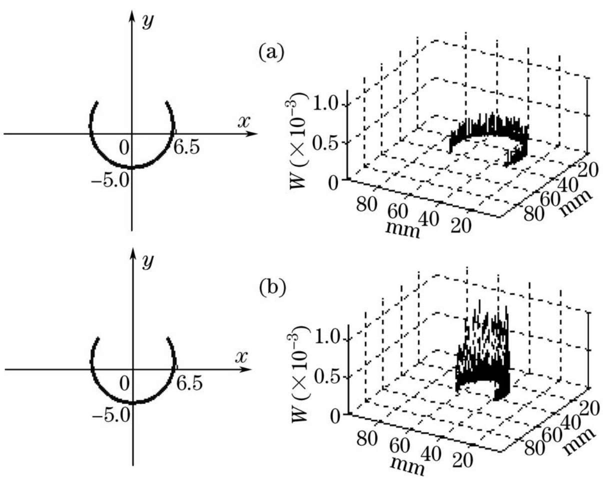

Fig. 5. The retinal images and energy distributions formed by square-edged design. (a): Squared-edged 1, the spatial location was in 6.31×4.97 mm^2, the intensity was 1.82×10^{-2} W; (b): Squared-edged 2, the spatial location was in 6.41×5.07 mm^2, the intensity was 4.07×10^{-2} W.

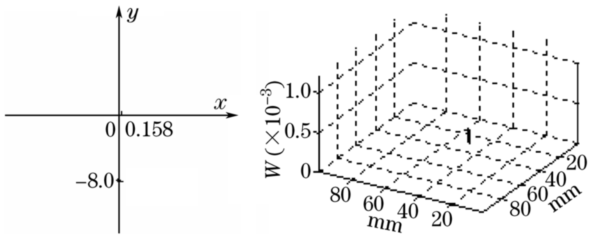

Fig. 6. The retinal images and energy distributions formed by round-/square-edged design. The spatial location was in 0.16×7.97 mm^2, the intensity was 2.42×10^{-4} W.

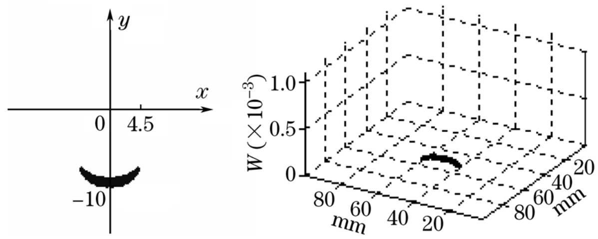

Fig. 7. The retinal images and energy distributions formed by "Σ"-edged design. The spatial location was in 4.40×10.25 mm^2, the intensity was 1.90×10^{-3} W.

Table 1. Intensity of Dysphotosia Connected to the Four IOL Edges (unit: W)

Square-Edged 1	Square-Edged 2	Round-/Square-edged	"Σ"-Edged
1.82×10^{-2}	4.07×10^{-2}	2.42×10^{-4}	1.90×10^{-3}

The results shown in Fig. 5 for the square edge designs are calculated with the glare source at 35° off-axis. However, the results shown in Fig. 6 for the round-/square-edged design are obtained only with the glare source at more than 35° off-axis, for example, 46°, where the glare rays can be reflected by the squared posterior edge and arrive at the retina (its ray paths shown as Fig. 3(c)). If the glare source is supposed at 35° off-axis, the result of dysphotopsia intensity in the retina is zero. The result shown in Fig. 7 for the "Σ"-edged design are also obtained with the glare source at 35° off-axis, where the cornea reflectivity is supposed to be 2.53%.

By the above analysis, it can be seen that the retinal images with the shape of a partial ring or thin arc are formed by the IOL edges. This may explain the reports of dysphotopsia related to flattened edges[8,9]. The intensity of dysphotosia connected to the four IOL edges is shown as Table 1.

From Table 1, it is shown that the intensity of arc-shaped image created by the "Σ" edge approach 1/10 that of the intensity with the square-edged design 1, about 1/21 that of the intensity with the square-edged design 2, and nearly 8 times that of the intensity with the round-/square-edged design. From above data shown by Figs. 5–7 and Table 1, the conclusion can be made: 1) the round-/square-edged design can lower incidence of reflect edge glare agreed with the reference 11; 2) the dysphotopsia intensity induced by the "Σ"-edged is larger than that by the round-/square-edged and less than that by square edges, but its spatial location is bigger and farther away from the center of retina than that of the round-/square-edged. Therefore, the potential of the "Σ"-edged design to lower dysphotopsia for pseudophakic patients is much more promising than the square-edged design, and less promising than the round-/square-edged design. The potential of the "Σ"-edged design to prevent PCO may be more promising than the square-edged design, according to the Ref. [1].

References

1. J. M. Marcantonio and G. F. Vrensen, Eye **13,** 484 (1999).

2. J. T. Holladay, A. Lang, and V. Portney, J. Cataract Refract Surg **25,** 748 (1999).
3. O. Nishi, K. Nishi, and K. Wickström, J. Cataract Refract Surg **26,** 1543 (2000).
4. M. F. Ellis, J. Cataract Refract Surg **27,** 1061 (2001).
5. W. Buehl, O. Findl, J. Akura, and T. Nagata, J. Cataract Refract Surg **28**, 1105 (2002).
6. D. R. Nixon, J. Cataract Refract Surg **30,** 2574 (2004).
7. R. Tester, N. L. Pace, M. Samore, and R. J. Olson, J. Cataract Refract Surg **26,** 810 (2000).
8. A. J. Kruger, J. Schauersberger, C. Abela, G. Schild, and M. Amon, J. Cataract Refract Surg **26,** 566 (2000).
9. J. C. Erie, M. H. Bandhauer, and V. Portney, J. Cataract Refract Surg **27,** 614 (2001).
10. S. Masket, E. Geraghy, and A. S. Crandall, J. Cataract Refract Surg **19,** 690 (1993).
11. A. Franchini, B. Zamma, and E. Vaccari, J. Cataract Refract Surg **29,** 342 (2003).